

8 February 2012

Charge Expulsion from Black Brane Horizons, and Holographic Quantum Criticality in the Plane¹

Eric D'Hoker and Per Kraus

Department of Physics and Astronomy
University of California, Los Angeles, CA 90095, USA
 dhoker@physics.ucla.edu; pkraus@physics.ucla.edu

Abstract

Quantum critical behavior in 2+1 dimensions is established via holographic methods in a 5+1-dimensional Einstein gravity theory with gauge potential form fields of rank 1 and 2. These fields are coupled to one another via a tri-linear Chern-Simons term with strength k . The quantum phase transition is physically driven by the expulsion of the electric charge from inside the black brane horizon to the outside, where it gets carried by the gauge fields which acquire charge thanks to the Chern-Simons interaction. At a critical value $k = k_c$, zero temperature, and any finite value of the magnetic field, the IR behavior is governed by a near-horizon Lifshitz geometry. The associated dynamical scaling exponent depends on the magnetic field. For $k < k_c$, the flow towards low temperature is governed by a Reissner-Nordstrom-like black brane whose charge and entropy density are non-vanishing at zero temperature. For $k > k_c$, the IR flow is towards the purely magnetic brane in AdS_6 . Its near-horizon geometry is $\text{AdS}_4 \times \mathbf{R}^2$, so that the entropy density vanishes quadratically with temperature, and all charge is carried by the gauge fields outside of the horizon.

¹This work was supported in part by NSF grant PHY-07-57702.

1 Introduction

Via the AdS/CFT correspondence, classical gravity can be used to model strongly interacting matter at finite temperature and finite charge density. Much activity in recent years has been devoted to finding classical solutions to various theories of gravity whose behavior bears some relation to interesting condensed matter systems. To the extent that strong coupling dynamics plays an important role in a given condensed matter system, the AdS/CFT correspondence is one of the few computational tools available. Holographic computations of thermodynamics and transport are relatively easy to carry out, since they reduce to questions involving classical gravity. See [1, 2] for reviews.

Quantum critical systems are particularly interesting to study in this regard. On the one hand, quantum criticality appears to be an important feature of various real world systems [3]. On the other hand, the inherent IR universality of such quantum critical points implies that it is meaningful to model these systems by the kinds of supersymmetric gauge theories that naturally arise in the AdS/CFT correspondence, even though their UV details may bear no relation to any realistic condensed matter system.

Experimentally, quantum critical points are found by tuning various control parameters, such as a pressure or a magnetic field, and one can attempt to map out a phase diagram in terms of these parameters. On the gravity side, it is possible to proceed similarly. One important driver of holographic quantum criticality is related to how charge is carried by such systems; in particular, the qualitative nature of the charge carriers can change under a variation of the control parameters, and this can signal a quantum critical point.

In the AdS/CFT correspondence, the density of charge in the boundary theory is equal to the amount of bulk electric flux that pierces the boundary. In the simplest bulk solution, the electrically charged Reissner-Nordstrom (RN) black brane, Gauss' law implies that these flux lines must all emanate from the horizon of the black brane, and so the charge carriers are hidden behind the horizon. The physical interpretation in the boundary theory is poorly understood, partly due to the fact that this RN solution has a large ground state entropy density.² An alternative scenario is for there to be a source on the right hand side of Gauss' law, in which case the electric flux lines can be generated in the bulk as one moves out radially. One way this can occur is if there is a condensate of a charged scalar field in the bulk; this spontaneously breaks the U(1) gauge symmetry and corresponds on the boundary to a holographic superfluid phase [5]. A second possibility is for there to exist a sea of charged particles in the bulk; solutions of this type have been studied in [6].

In the present paper, we are primarily interested in yet another possibility, in which Gauss' law is modified by Chern-Simons interactions. In the presence of a Chern-Simons

²It has been suggested, e.g. in [4], that one should think of these as fractionalized phases of matter, in analogy with the fact that horizons are known to describe the deconfined phases of gauge theories in the AdS/CFT correspondence.

term, gauge fluxes can themselves carry charge, and this allows for charge to be located outside an event horizon in the absence of explicit charged particles, and without breaking the $U(1)$ symmetry. This mechanism played a key role in the magnetic quantum critical points studied in [7, 8, 9] (see [10] for another example of magnetic quantum criticality in a holographic setting). There, the bulk theory was five-dimensional Einstein-Maxwell-Chern-Simons theory. Solutions were obtained that are dual to a boundary gauge theory at finite charge density and external magnetic field. In the bulk, the simultaneous presence of electric and magnetic fluxes activated the Chern-Simons term, allowing bulk charge to be carried in the manner described above. The strength of this effect was varied by changing either the Chern-Simons level k or the value of the magnetic field B , and a rich phase structure was uncovered. Most interestingly, for sufficiently large k , a magnetically tuned quantum critical point with nontrivial scaling properties was discovered, resembling real world systems in a number of ways [7].

The critical theories studied in [7, 8] are effectively 1+1 dimensional: while the underlying gauge theory is defined in $D=3+1$, at the critical point massless propagation takes place along a single spatial direction. In the bulk, this was seen from the existence of a near-horizon geometry of the form $WAdS_3 \times \mathbf{R}^2$, where $WAdS_3$ is a “null warped” deformation of AdS_3 space [11, 12]. The \mathbf{R}^2 was supported by the nonzero magnetic field. While quantum criticality in 1+1 dimensions is certainly important, it is also interesting to generalize to higher dimensions. Particular interest attaches to the case of 2+1 dimensions, which in the real world is relevant to various layered materials such as the cuprates. Our goal in the present work is thus to find a magnetic quantum critical point in 2+1 dimensions, driven by the presence of Chern-Simons terms.

1.1 Overview of the set-up

The simplest setup exhibiting the desired behavior appears to be six-dimensional gravity coupled to a one-form potential A and a two-form potential C . Assuming gauge invariance under $A \rightarrow A + d\Lambda_A$ and $C \rightarrow C + d\Lambda_C$, the most general two-derivative action is,

$$S = -\frac{1}{16\pi G_6} \int d^6x \sqrt{g} \left(R - \frac{20}{L^2} + F^{MN} F_{MN} + \frac{1}{3} G^{MNP} G_{MNP} \right) + S_{CS} + S_{\text{bndy}} \quad (1.1)$$

with the Chern-Simons (CS) term S_{CS} given by,

$$S_{CS} = \frac{k}{4\pi G_6} \int C \wedge F \wedge F \quad (1.2)$$

Here $F = dA$ and $G = dC$ are the two-form and three-form field strengths respectively. While such an action can plausibly arise within string theory, for the time being we will

regard this as the result of a bottom-up construction.³ Although the dual boundary theory is defined in 4+1 dimensions,⁴ as discussed above our primary interest is in finding solutions corresponding to quantum criticality in 2+1 dimensions. This is achieved by introducing a magnetic field, which acts to freeze out two of the spatial dimensions in the IR.

To turn on a nonzero charge density ρ and magnetic field B we consider a two-form field strength of the form

$$F = E(r) dr \wedge dt + B dx^3 \wedge dx^4 \quad (1.3)$$

The value of the charge density ρ is read off from the asymptotic behavior of E , namely $\rho \sim r^4 E(r)$ as $r \rightarrow \infty$. The CS term induces a nonzero three-form field strength,

$$G = G_1(r) dr \wedge dx^1 \wedge dx^2 \quad (1.4)$$

The full solution is taken to be translationally invariant along all boundary directions, as well as rotationally invariant in the $x^{1,2}$ and $x^{3,4}$ planes. The form-field equations of motion exhibit a source in Gauss' law due to the CS term,

$$\begin{aligned} d * F - 2k F \wedge G &= 0 \\ d * G + k F \wedge F &= 0 \end{aligned} \quad (1.5)$$

In particular, the product BG_1 acts as a charge density sourcing E .

1.2 Summary of the results

Given this setup, we can try to characterize the zero temperature solutions of this theory as a function of the charge density ρ , magnetic field B , and Chern-Simons level k . Actually, due to scale invariance there are really only two parameters to vary: the dimensionless parameter k and the dimensionless ratio,

$$\hat{B} = \frac{B}{\sqrt{\rho}} \quad (1.6)$$

One way to summarize our results is to give the low temperature behavior of the entropy density s for various values of \hat{B} and k . Let us first note two special cases that are easy to understand. For $\hat{B} = 0$ the solution is just the electric RN black brane, with a finite entropy density at zero temperature. The other extreme is $\hat{B} = \infty$, attained with $E = \rho = 0$. In

³A related theory with two-form and three-form potentials and Chern-Simons terms is obtained from massive IIA supergravity [15], and admits solutions with a four-dimensional Lifshitz factor [16, 17], similar to what we find below.

⁴CFTs in 4+1 dimensions are rare, but not unheard of [18].

this case we find a six-dimensional version of the magnetic brane solution studied in [13] for five dimensions. The solution develops a near-horizon $\text{AdS}_4 \times \mathbf{R}^2$ geometry which connects to the asymptotic AdS_6 . In both of these cases the three-form field strength G vanishes identically, and the Chern-Simons term plays no role.

For finite nonzero values of \hat{B} we find that the qualitative behavior depends on the magnitude of k relative to its critical value $k_c = 1/\sqrt{3}$. We discuss the three cases in turn.

1.2.1 The case $k < k_c$

Solutions in this regime can be thought of as deformed versions of the purely electric RN solution. At $\hat{B} = 0$, we have precisely the RN solution, as G_1 vanishes and the CS term plays no role. At zero temperature, the near-horizon region becomes $\text{AdS}_2 \times \mathbf{R}^4$, and the zero temperature entropy density is proportional to the charge density: $s \propto \rho$. For this RN solution, all of the charge is hidden behind the horizon.

Turning on nonzero \hat{B} activates G_1 and the CS term. At zero temperature the near-horizon region again exhibits an $\text{AdS}_2 \times \mathbf{R}^4$, but now only a finite fraction of the charge is hidden behind the horizon, with the remainder carried outside the horizon by the flux term BG_1 . As k and/or \hat{B} is increased, this effect becomes more pronounced, with more charge transferred from behind the horizon to outside, as illustrated in figure 1. The transfer becomes complete as k reaches its critical value k_c , at which point there is a quantum phase transition. For $k < k_c$, all of these solutions have a nonzero ground state entropy density.

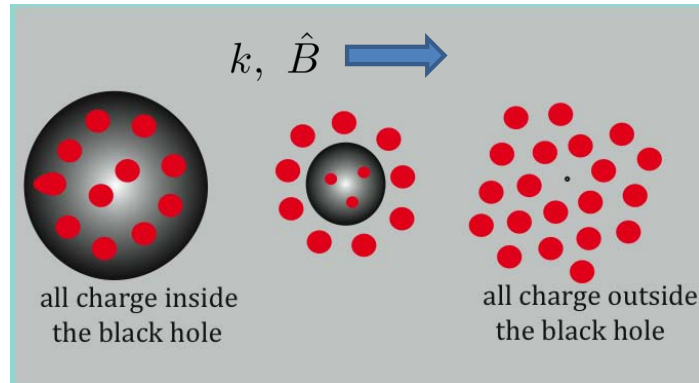


Figure 1: As k and \hat{B} are increased (indicated by the blue arrow), the charge inside the horizon of the black hole gets expelled and carried by the gauge fields outside the horizon.

1.2.2 The case $k > k_c$

Here the solutions are generalizations of the purely magnetic brane solution obtained for $E = G_1 = 0$. The purely magnetic solution interpolates between a near-horizon $\text{AdS}_4 \times \mathbf{R}^2$ region and AdS_6 asymptotically, and is the analog of the 5D magnetic brane solution studied in [13]. The low temperature entropy density behaves like that of a D=2+1 Lorentz invariant CFT, and exhibits the expected $s \propto T^2$. At small but nonzero temperature, the near-horizon region has AdS_4 replaced by an AdS_4 Schwarzschild black brane.

Turning on nonzero charge density changes the details, but the qualitative picture remains. The zero temperature solutions always exhibit a near-horizon $\text{AdS}_4 \times \mathbf{R}^2$ region and the entropy density is quadratic in the temperature. The dependence on \hat{B} and k can be seen in the behavior of the prefactor,

$$\hat{s} \sim A(k, \hat{B}) \hat{T}^2 \quad (1.7)$$

where we now work in terms of dimensionless quantities, referred to with hats, and to be defined precisely in (3.29). It is interesting to explore the behavior of $A(k, \hat{B})$ as \hat{B} tends to 0, since precisely at $\hat{B} = 0$ (obtained for $B = 0$ and $\rho \neq 0$) we arrive back at the purely electric RN solution with its finite entropy density ground state. The coefficient $A(k, \hat{B})$ must therefore exhibit a singularity, and indeed we find the following behavior, as $\hat{B} \rightarrow 0$,

$$A(k, \hat{B}) \sim c(k) \exp \left\{ \frac{d(k)}{\hat{B}^2} \right\} \quad (1.8)$$

for real positive functions $c(k)$ and $d(k)$. We present clear numerical evidence for the simple but distinctive analytical behavior of $A(k, \hat{B})$ (and for $d(k)$ as explained below), even though at present the corresponding analytical derivations are not available.

For $k > k_c$ we therefore find that the ground state entropy density of the purely electric RN solution is removed by the presence of any nonzero magnetic field B . For any finite B , the entropy density will always go to zero quadratically in T as $T \rightarrow 0$. The finite ground state entropy density of the RN solution thus requires a fine tuning, since it is removed by turning on an arbitrarily small magnetic field. It is instructive to compare this to the behavior of the analogous charged magnetic brane solutions in AdS_5 studied in [14]. There, we conjectured, based on preliminary numerical analysis, that the AdS_5 RN ground state entropy density would similarly be removed by the presence of any finite magnetic field. However, subsequent high-precision numerical work [7] and analytical calculations [8] revealed that the magnetic field needed to be larger than a value B_c to achieve this. So in this sense the effect of the magnetic field appears to be stronger in the AdS_6 case as compared to AdS_5 .

The function $A(k, \hat{B})$ is also singular as k approaches k_c from above. Numerical analysis shows that the coefficient $d(k)$ behaves as

$$d(k) \sim \frac{d_0}{k^2 - k_c^2} \quad (1.9)$$

to remarkably good accuracy in the range $k_c < k < 1.2$. Here, d_0 is a constant of order 1. This again signals a quantum phase transition at k_c , to which we now turn.

1.2.3 The case $k = k_c$

Numerical analysis at $k = k_c$ indicates that the low temperature entropy density scales to zero as a \hat{B} -dependent power of temperature,

$$s \propto T^{2/z} \quad z = z(\hat{B}) \rightarrow \begin{cases} \infty & \text{as } \hat{B} \rightarrow 0 \\ 1 & \text{as } \hat{B} \rightarrow \infty \end{cases} \quad (1.10)$$

A plot of $z(\hat{B})$ will be shown in figure 6. Such a behavior is characteristic of a 2+1 dimensional scale invariant theory with dynamical critical exponent $z = z(\hat{B})$. Indeed, precisely at $k = k_c$ the field equations admit a new near-horizon geometry of the form $\text{Lif}_4 \times \mathbf{R}^2$, where Lif_4 is a 3+1 dimensional Lifshitz solution [19] with dynamical exponent z . Explicitly,

$$\begin{aligned} ds^2 &= \frac{dr^2}{u_0 r^2} - u_0 r^2 dt^2 + r^{2/z} \left((dx^1)^2 + (dx^2)^2 \right) + \left((dx^3)^2 + (dx^4)^2 \right) \\ F &= q_0 dr \wedge dt + b_0 dx^3 \wedge dx^4 \\ G &= -\frac{q_0}{k b_0 z} r^{2/z-1} dr \wedge dx^1 \wedge dx^2 \end{aligned} \quad (1.11)$$

In terms of z restricted to the range $1 \leq z \leq \infty$, as is required for all fields to be real valued, the values of q_0 and b_0 are fixed as

$$q_0^2 = \frac{10z(z-1)}{(z+2)^2} \quad b_0^2 = \frac{30z}{(z+2)^2} \quad (1.12)$$

The parameters q_0 and b_0 represent the near-horizon value of the electric charge and magnetic field respectively, and are related to asymptotic quantities measured at the AdS_6 boundary by the full interpolating solution. There is thus a nontrivial expression for \hat{B} in terms of z , or equivalently $z(\hat{B})$, whose form is only known numerically; see figure 6 below.

Numerical analysis shows that as the temperature is lowered at $k = k_c$ a near-horizon region of the form (1.11) indeed develops and controls the low temperature thermodynamics. Also, as \hat{B} varies from 0 to ∞ , the dynamical exponent z smoothly varies between ∞ and 1, so that the family of Lifshitz geometries interpolates between $\text{AdS}_2 \times \mathbf{R}^4$ and $\text{AdS}_4 \times \mathbf{R}^2$.

In figure 2, we display representative numerical data that illustrate the points made above. In the left panel (b, q) denote the values of the electric and magnetic fields at the horizon (in a particular coordinate system described in the text). By varying the temperature for a fixed value of \hat{B} we obtain curves in (b, q) space. The curves emanate from the origin, which

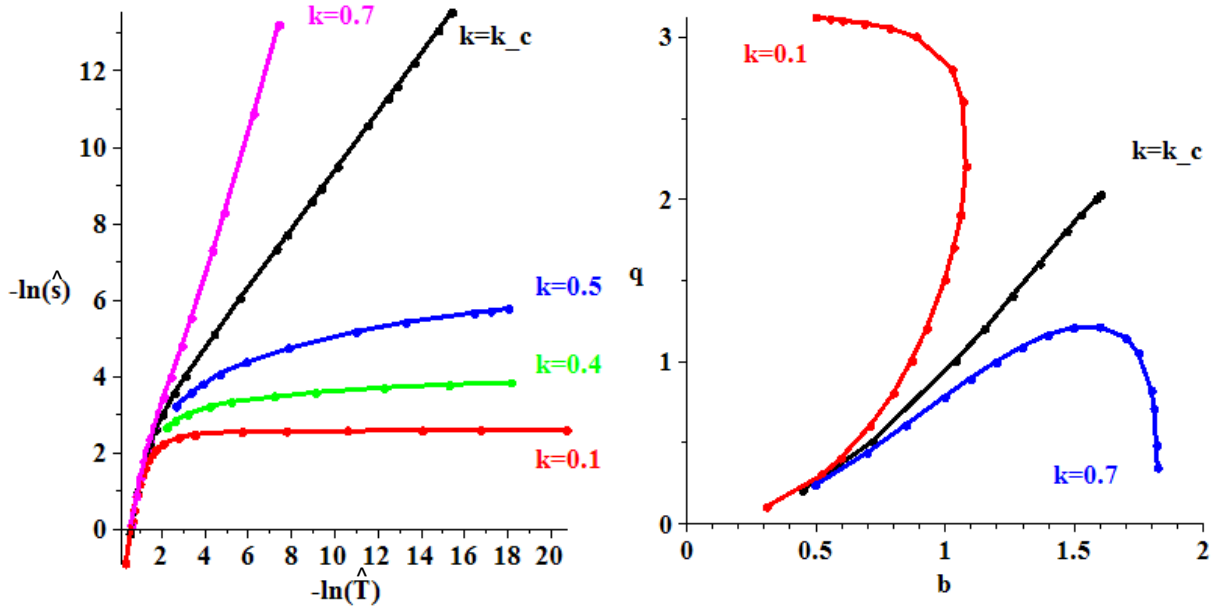


Figure 2: Left panel: Entropy density \hat{s} versus temperature \hat{T} for selected values of k . Right panel: Flows towards low temperature of the horizon data q and b , for fixed $\hat{B} = 1$, for $k = 0.1$ (red dots), $k = k_c$ (black dots), and $k = 0.7$ (magenta dots).

corresponds to the high temperature regime. As the temperature is lowered, the curves either flow to the electric fixed point at $b = 0$ for $k < k_c$; to the magnetic fixed point at $q = 0$ for $k > k_c$; or to a point on a critical curve with nonzero q and b for $k = k_c$. In the right panel we show the corresponding behavior of the entropy density as a function of temperature. As $T \rightarrow 0$, the entropy density either goes to a finite value ($k < k_c$); to zero quadratically in temperature ($k > k_c$); or to zero with a \hat{B} dependent power between 0 and 2 ($k = k_c$).

Examining the overall picture, summarized in figure 3, the story is quite similar to that in the AdS_5 case, except that the roles of k and B are, in a sense, interchanged. In the AdS_5 case a critical point was reached by tuning B to B_c , and at the critical point the dynamical exponent z depended on k . But in the AdS_6 case studied here, the critical point is reached by tuning k , and at the critical point the dynamical exponent varies with B . The other major distinction is, of course, that for AdS_5 the critical theory was 1+1 dimensional, while in the AdS_6 case it is 2+1 dimensional.

A model with related behavior was studied in [20]. There also, transitions were found between finite and zero entropy density states at zero temperature, mediated by the appearance of a Lifshitz near horizon geometry.

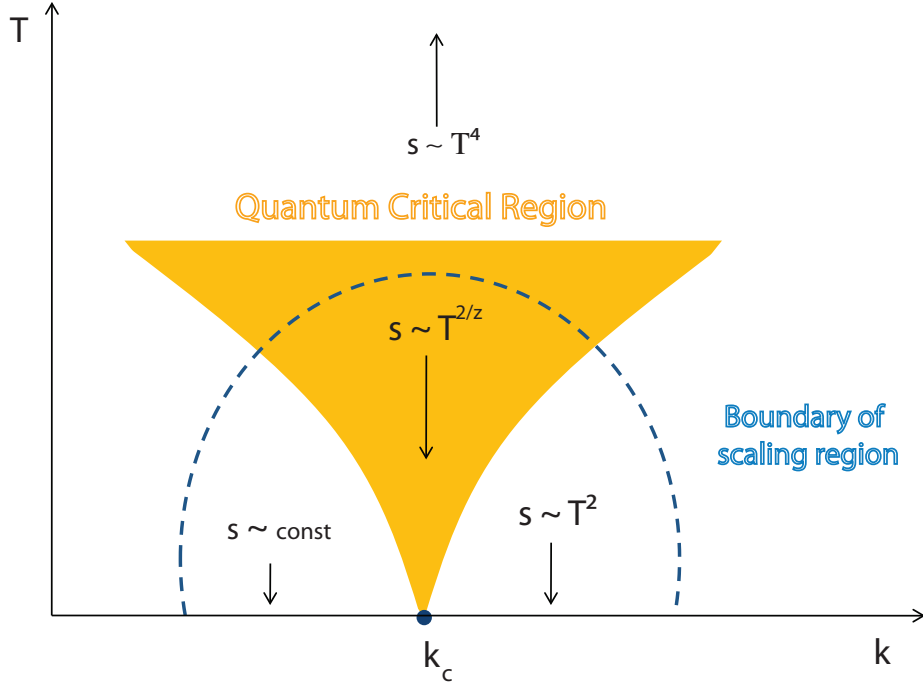


Figure 3: Phase diagram of entropy density s versus k for all finite \hat{B} .

1.3 Organization

The remainder of this paper is organized as follows. In section 2, we present a general discussion of candidate theories for holographic quantum critical behavior in 2+1 dimensions, built on Einstein gravity plus gauge fields of various ranks. The theory of gauge field potentials of rank 1 and 2 in six space-time dimensions with a Chern-Simons coupling, considered in this paper, emerges as one of the simplest such models. In section 3, a detailed discussion of the action, field equations, symmetries, suitable Ansatz, and reduced field equations for the study of thermodynamic quantities is presented. In section 4, the special solutions corresponding to the well-known AdS_6 Reissner-Nordstrom black brane, and the novel purely magnetic brane in AdS_6 are derived. The critical value of $k = k_c$ is inferred from the behavior of small fluctuations around the purely magnetic brane. The existence of a Lifshitz near-horizon geometry at $k = k_c$ is shown in section 5, its extension to a full fledged six-dimensional solution is derived numerically, while an analytical derivation of the small fluctuation spectrum around Lifshitz is deferred to Appendix A. In section 6, a detailed discussion is presented of our numerical results, and their matching with analytical calculations when available (with further details explained in Appendix B). Finally, the quantum critical behavior of the system is discussed in section 7.

2 Candidates with p -form fields

The holographic model for quantum critical behavior in 1+1 dimensions based on 4+1-dimensional Einstein-Maxwell-Chern-Simons [7, 8] draws on a number of fundamental dynamical properties.

1. The presence of a constant background magnetic field induces an IR flow towards a lower-dimensional AdS theory;
2. The gauge field can carry charge thanks to the Chern-Simons interaction. This mechanism permits charge to be expelled from the inside of the black brane horizon to the outside where it is carried by the gauge field.
3. Tri-linearity of the Chern-Simons action supplies the IR theory with an effective Chern-Simons theory for the low-energy fields.

The goal of this paper is to generalize and extend this construction to space-times where quantum criticality takes place in field theories of dimension higher than 1+1. To do so, we shall want to respect the basic tenets above. Given these assumptions, which theories can we construct, while maintaining the basic assumption that no scalar fields be present?

2.1 Gravity models with a single form-field

The Einstein-Maxwell-Chern-Simons theory of [7, 8], formulated in terms of a single 1-form field potential, admits a straightforward generalization to a theory with a single p -form field C whose field strength form is denoted by $G = dC$. The corresponding action is given by,

$$S = -\frac{1}{16\pi G_D} \int d^D x \sqrt{g} \left(R - \Lambda + |G|^2 \right) + S_{\text{CS}} \quad (2.1)$$

where Λ is the cosmological constant, S_{CS} the Chern-Simons term given by,

$$S_{\text{CS}} = \frac{k}{4\pi G_D} \int C \wedge G \wedge G \quad (2.2)$$

and the boundary action has been suppressed. Matching of dimensions requires $D = 3p + 2$. The Einstein-Maxwell-Chern-Simons theory of [7, 8] corresponds to $p = 1$. When $p > 1$, we assume that G has a boundary magnetic field that generates a flow from $\text{AdS}_D = \text{AdS}_{3p+2}$ in the UV to $\text{AdS}_{D-p-1} = \text{AdS}_{2p+1}$ in the IR. For $p = 2$, we have $D = 8$ and a flow towards AdS_5 , while for $p = 3$, we have $D = 11$ and flow towards AdS_7 . The latter case might be of special interest as arising from M-theory on a S^4 sphere with magnetic field. All of these schemes may be interesting, but still they lack the presence of the fundamental electro-magnetic field.

2.2 Gravity models with two form-fields

Gravity models with two different form potential fields A and C , respectively of ranks p' and p , and field strengths $F = dA$ and $G = dC$, offer a further extension of the Einstein-Maxwell-Chern-Simons models of [7, 8].⁵ The general action is as follows,

$$S = -\frac{1}{16\pi G_D} \int d^D x \sqrt{g} (R - \Lambda + |F|^2 + |G|^2) + S_{\text{CS}} \quad (2.3)$$

where Λ is the cosmological constant. All possible tri-linear Chern-Simons terms are,

$$\begin{aligned} S_{\text{CS}}^{AAA} &= \frac{k_1}{4\pi G_D} \int A \wedge F \wedge F & D = 3p' + 2 \\ S_{\text{CS}}^{AAC} &= \frac{k_2}{4\pi G_D} \int A \wedge F \wedge G & D = 2p' + p + 2 \\ S_{\text{CS}}^{ACC} &= \frac{k_3}{4\pi G_D} \int A \wedge G \wedge G & D = p' + 2p + 2 \\ S_{\text{CS}}^{CCC} &= \frac{k_4}{4\pi G_D} \int C \wedge G \wedge G & D = 3p + 2 \end{aligned} \quad (2.4)$$

In the presence of two different form fields of the same rank $p = p'$, all of the above Chern-Simons terms are allowed for $D = 3p + 2$, and the theory is characterized by 4 independent dimensionless couplings k_1, k_2, k_3, k_4 . On the other hand, if $p \neq p'$, and we take $p' < p$, then for given D only a single one of the above Chern-Simons couplings can occur.

Assuming that one of the potentials A is electro-magnetic, we set $p' = 1$, and $p > 1$. For $p = 1$ we recover the $D = 5$ theory considered in [7, 8] except now with two gauge fields and a mixed Chern-Simons term; theories of this type were studied in [22, 23]. For $D > 5$, each value of $p \geq 2$ yields a unique theory with Chern-Simons term S_{CS}^{AAC} in dimension $D = 4 + p$, and a unique theory with Chern-Simons term S_{CS}^{ACC} with dimension $D = 3 + 2p$. The next simplest case has $p = 2$, $D = 6$ and Chern-Simons term S_{CS}^{AAC} and is the one considered here. Another interesting case is $p = 2$, $D = 7$ and Chern-Simons term S_{CS}^{ACC} .

3 The Einstein-Maxwell-two-form-field system

In this section, we present the Einstein-Maxwell-two-form-field system in detail, including the action and field equations. To study thermodynamics in the presence of a uniform background magnetic field and electric charge density, we focus on solutions which are invariant under translations, and certain rotations, of the boundary theory. We obtain the corresponding Ansätze and reduced field equations.

⁵We will be assuming invariance (up to boundary terms) of the action under the gauge invariance $A \rightarrow A + d\Lambda_A$, $C \rightarrow C + d\Lambda_C$, although further generalizations could be envisaged as well.

3.1 Field contents and field equations

The fundamental fields of the 6-dimensional theory are: the metric g_{MN} , the Maxwell field A_M , and the 2-form field $C_{MN} = -C_{NM}$. The action consists of the Einstein-Hilbert term, standard kinetic terms for the fields A and C , and the only possible Chern-Simons term afforded by this structure,⁶

$$S = -\frac{1}{16\pi G_6} \int d^6x \sqrt{g} \left(R - \frac{20}{L^2} + F^{MN} F_{MN} + \frac{1}{3} G^{MNP} G_{MNP} \right) + S_{\text{CS}} + S_{\text{bdy}} \quad (3.1)$$

with the Chern-Simons term S_{CS} given by,

$$S_{\text{CS}} = \frac{k}{4\pi G_6} \int C \wedge F \wedge F \quad (3.2)$$

The explicit form of the boundary action S_{bdy} will not be needed. Here, G_6 is Newton's constant in 6 dimensions, L sets the scale for the cosmological constant, and k is the sole remaining dimensionless coupling. The action (3.1) is invariant under the gauge invariance $A \rightarrow A + d\Lambda_A$, $C \rightarrow C + d\Lambda_C$, up to a boundary term generated by S_{CS} ; in fact, (3.1) is the most general two-derivative action with this property. The field strength and potential forms, and their components, are related as follows,

$$\begin{aligned} A &= A_M dx^M & F &= dA = \frac{1}{2} F_{MN} dx^M \wedge dx^N \\ C &= \frac{1}{2} C_{MN} dx^M \wedge dx^N & G &= dC = \frac{1}{6} G_{MNP} dx^M \wedge dx^N \wedge dx^P \end{aligned} \quad (3.3)$$

Einstein's equations may be cast in the following form,

$$R_{MN} = -2F_{MP}F_N{}^P - G_{MPQ}G_N{}^{PQ} + g_{MN} \left(\frac{5}{L^2} + \frac{1}{4} F_{PQ}F^{PQ} + \frac{1}{6} G_{PQR}G^{PQR} \right) \quad (3.4)$$

Note that the contribution of the F -field is traceless in 4 dimensions while that of the G -field is traceless in 6 dimensions, as we should expect. The Maxwell equations in the presence of the 2-form field C are given by the Bianchi identity $dF = 0$, together with the field equation,

$$\nabla_M F^{MN} = -\frac{k}{2\sqrt{g}} \varepsilon^{MNPQRS} F_{PQ} \partial_M C_{RS} \quad (3.5)$$

⁶Throughout, Einstein indices range over $M, N, P = 0, 1, 2, 3, 4, 5$, and we define $g = -\det(g_{MN})$. Isolating the holographic radial direction r , and the time direction 0, we adopt the following convention for the orientation, $\varepsilon_{r01234} = 1$. Expressed in Einstein indices, the dual $\star G$ of a p -form G with components $G_{M_1 \dots M_p}$, is defined by $(\star G)_{N_1 \dots N_{6-p}} = \frac{\sqrt{g}}{p!} \varepsilon_{M_1 \dots M_p N_1 \dots N_{6-p}} G^{M_1 \dots M_p}$.

The 2-form field equations in the presence of the Maxwell field are given by the Bianchi identity $dG = 0$, together with the field equation,

$$\nabla_P G^{PMN} = \frac{k}{4\sqrt{g}} \varepsilon^{MNPQRS} F_{PQ} F_{RS} \quad (3.6)$$

In form notation, these equations become,

$$\begin{aligned} d * F - 2kF \wedge G &= 0 \\ d * G + kF \wedge F &= 0 \end{aligned} \quad (3.7)$$

Henceforth, we set $L = 1$, and refer to the fields F, G as the *gauge fields* of the system, and to (3.7) as the *gauge field equations*.

3.2 Ansatz with translation and rotation symmetries

The precise symmetry requirements will depend upon the physical questions addressed. Throughout, we shall be interested in thermodynamic quantities (postponing problems involving correlators to later work) evaluated in the presence of a uniform magnetic $F_{34} = B$ field in the x^3, x^4 directions, as well as a physical electric charge density ρ . Therefore, the natural symmetries to be imposed will always include the following,⁷

1. Translations in t, x^1, x^2, x^3, x^4 ;
2. Rotations in the $x^1 x^2$ -plane;
3. Rotations in the $x^3 x^4$ -plane.

The Ansatz for the general metric invariant under the above symmetries is given as follows,

$$ds^2 = \frac{dr^2}{U} - U dt^2 + e^{2V_1} \left((dx^1)^2 + (dx^2)^2 \right) + e^{2V_2} \left((dx^3)^2 + (dx^4)^2 \right) \quad (3.8)$$

This metric is expressed in a specific gauge choice for the holographic coordinate r in which $g_{rr} g_{tt} = -1$. The functions U, V_1, V_2 depend only on r by translation invariance. Subject to the same symmetries, the gauge field Ansätze are given by,

$$\begin{aligned} F &= E dr \wedge dt + B_1 dx^1 \wedge dx^2 + B_2 dx^3 \wedge dx^4 \\ G &= (G_1 dr + G_2 dt) \wedge dx^1 \wedge dx^2 + (G_3 dr + G_4 dt) \wedge dx^3 \wedge dx^4 \end{aligned} \quad (3.9)$$

⁷The field equations are also invariant under the sign-reversal of F . We will not be led to impose this symmetry on our holographic solutions, since we know that this discrete symmetry will be broken by a finite electric charge density.

Translation symmetry again restricts all coefficients to be independent of x^0, x^1, x^2, x^3, x^4 . To satisfy the Bianchi identities $dF = dG = 0$ the coefficients B_1, B_2, G_2, G_4 must be independent of r . The remaining coefficients E, G_1, G_3 are generally functions of r .

Throughout, one of the magnetic fields will be kept non-zero, and used to generate the RG flow from AdS_6 to a 2+1-dimensional IR boundary theory. The other magnetic field, which lives in this 2+1-dimensional IR theory, will be set to zero for simplicity. We choose,

$$B_1 = 0 \qquad B_2 = B \qquad (3.10)$$

where $B \neq 0$. (Note that for $B_1 = B_2$, exact solutions may be found which are closely related to the dyonic AdS_4 Reissner-Nordstrom black brane [13].)

3.3 General reduced gauge field equations

It is straightforward to compute the reduced field equations for the gauge fields, and we find,

$$\begin{aligned} M1 \quad & 0 = \left(E e^{2V_1 + 2V_2} \right)' + 2k B G_1 \\ M2 \quad & 0 = \left(G_1 U e^{2V_2 - 2V_1} \right)' + 2k B E \\ M3 \quad & 0 = \left(G_3 U e^{2V_1 - 2V_2} \right)' \end{aligned} \qquad (3.11)$$

as well as the relation,

$$2k B G_2 = 0 \qquad (3.12)$$

Note that the Bianchi identities were solved already in the preceding subsection. Since we are assuming throughout that $kB \neq 0$ the field equations imply $G_2 = 0$. Furthermore, equation $M3$ may be integrated once, to obtain,

$$G_3(r) = \frac{c_3}{U(r)} e^{-2V_1(r) + 2V_2(r)} \qquad (3.13)$$

where c_3 is an arbitrary integration constant.

3.4 General reduced Einstein equations

The reduced Einstein equations were computed using Maple. The equation for the R_{rt} component is simply given by,

$$2G_1 G_2 e^{-4V_1} + G_3 G_4 e^{-4V_2} = 0 \qquad (3.14)$$

Since we have already deduced the relation $G_2 = 0$ from the reduced gauge field equations, we conclude that we must have $G_3 G_4 = 0$. With the help of (3.11), this condition becomes a relation between constants,

$$c_3 G_4 = 0 \quad (3.15)$$

Eliminating $G_3(r)$ using equation (3.11), and replacing the R_{tt} equation by the combination $(R_{rr} - R_{tt})/(4U)$, we find the following reduced Einstein equations,

$$\begin{aligned} E1 \quad & 0 = V_1'' + (V_1')^2 + V_2'' + (V_2')^2 + G_1^2 e^{-4V_1} \\ & \quad + U^{-2} (c_3^2 e^{-4V_1} + G_4^2 e^{-4V_2}) \\ E2 \quad & 0 = UV_1'' + U'V_1' + 2UV_1'^2 + 2UV_1'V_2' - 5 + \frac{1}{2}E^2 - \frac{1}{2}B^2 e^{-4V_2} \\ & \quad + UG_1^2 e^{-4V_1} - U^{-1} (c_3^2 e^{-4V_1} - G_4^2 e^{-4V_2}) \\ E3 \quad & 0 = UV_2'' + U'V_2' + 2UV_2'^2 + 2UV_2'V_1' - 5 + \frac{1}{2}E^2 + \frac{3}{2}B^2 e^{-4V_2} \\ & \quad - UG_1^2 e^{-4V_1} + U^{-1} (c_3^2 e^{-4V_1} - G_4^2 e^{-4V_2}) \\ E4 \quad & 0 = U'' + 2U'(V_1' + V_2') - 10 - 3E^2 - B^2 e^{-4V_2} \\ & \quad - 2UG_1^2 e^{-4V_1} - 2U^{-1} (c_3^2 e^{-4V_1} + G_4^2 e^{-4V_2}) \end{aligned} \quad (3.16)$$

The constraint equation is obtained as the combination $E2 + E3 - UE1$, and is given by

$$\begin{aligned} CON \quad & 0 = U'(V_1' + V_2') + U(V_1'^2 + V_2'^2 + 4V_1'V_2') - 10 + E^2 + B^2 e^{-4V_2} \\ & \quad - UG_1^2 e^{-4V_1} - U^{-1} (c_3^2 e^{-4V_1} + G_4^2 e^{-4V_2}) \end{aligned} \quad (3.17)$$

Using Maple, one can check that the derivative of the constraint equation CON vanishes in view of the other Einstein and gauge field equations.

3.5 Reduced equations for solutions with a smooth horizon

We look for a smooth finite temperature horizon, at which U has a single zero. Other solutions will certainly exist, but it seems plausible that only solutions with smooth horizons are of physical interest to us. From Einstein equation $E1$ in (3.16) it is clear that we need $c_3 = G_4 = 0$ if we are to assume that V_1 , V_2 , and G_1 are smooth functions at the horizon. This condition, of course, automatically solves the Einstein equation (3.15). With this restriction, the gauge fields simplify as follows,

$$\begin{aligned} F &= E(r)dr \wedge dt + Bdx^3 \wedge dx^4 \\ G &= G_1(r)dr \wedge dx^1 \wedge dx^2 \end{aligned} \quad (3.18)$$

Equation $M3$ in (3.11) is satisfied automatically, while equations $M1$ and $M2$ are unchanged; we repeat them here for later convenience.

$$\begin{aligned} M1 \quad & 0 = \left(E e^{2V_1+2V_2} \right)' + 2k B G_1 \\ M2 \quad & 0 = \left(G_1 U e^{2V_2-2V_1} \right)' + 2k B E \end{aligned} \quad (3.19)$$

With $c_3 = G_4 = 0$, the reduced Einstein equations of (3.16) simplify and become,

$$\begin{aligned} E1 \quad & 0 = V_1'' + (V_1')^2 + V_2'' + (V_2')^2 + G_1^2 e^{-4V_1} \\ E2 \quad & 0 = UV_1'' + U'V_1' + 2UV_1'^2 + 2UV_1'V_2' - 5 + \frac{1}{2}E^2 - \frac{1}{2}B^2 e^{-4V_2} + UG_1^2 e^{-4V_1} \\ E3 \quad & 0 = UV_2'' + U'V_2' + 2UV_2'^2 + 2UV_2'V_1' - 5 + \frac{1}{2}E^2 + \frac{3}{2}B^2 e^{-4V_2} - UG_1^2 e^{-4V_1} \\ E4 \quad & 0 = U'' + 2U'(V_1' + V_2') - 10 - 3E^2 - B^2 e^{-4V_2} - 2UG_1^2 e^{-4V_1} \end{aligned} \quad (3.20)$$

while the constraint is given by,

$$CON \quad 0 = U'(V_1' + V_2') + U(V_1'^2 + V_2'^2 + 4V_1'V_2') - 10 + E^2 + B^2 e^{-4V_2} - UG_1^2 e^{-4V_1} \quad (3.21)$$

3.6 Horizon Data

For the purpose of carrying out numerical analysis, we need to fix the remaining freedom in the choice of coordinates. We put the horizon at $r = 0$. Using the freedom to rescale time t (while compensating by a rescaling of r), as well as $x^{1,2}$ and $x^{3,4}$, we shall normalize the components of the metric by setting,

$$U(0) = V_1(0) = V_2(0) = 0 \quad U'(0) = 1 \quad (3.22)$$

and use the following notation for the components of the gauge fields,

$$B = b \quad E(0) = q \quad G_1(0) = g \quad (3.23)$$

Solving $E2$, $E3$, CON , and $M2$ at the horizon produces expressions for the derivatives $V_1'(0)$, $V_2'(0)$, as well as a relation giving g in terms of the other data,

$$\begin{aligned} g = -2kbq \quad & V_1'(0) = 5 - \frac{1}{2}q^2 + \frac{1}{2}b^2 \\ & V_2'(0) = 5 - \frac{1}{2}q^2 - \frac{3}{2}b^2 \end{aligned} \quad (3.24)$$

Thus, the free parameters, as specified at the horizon, are now b and q . We should find a unique solution for each choice of (b, q) , though the requirement of global regularity will restrict the allowed range of these parameters.

3.7 Asymptotic data and physical quantities

For every regular solution, with specified values of (b, q) , the asymptotic behavior as $r \rightarrow \infty$ will approach the geometry of the boundary of AdS_6 . The $r \rightarrow \infty$ asymptotic behavior of the components of the metric takes the familiar AdS_6 form,

$$\frac{U(r)}{r^2} \rightarrow 1 \quad \frac{e^{2V_1(r)}}{r^2} \rightarrow v_1 \quad \frac{e^{2V_2(r)}}{r^2} \rightarrow v_2 \quad (3.25)$$

The asymptotics of the gauge field strengths fix the physical charges of the boundary theory,

$$E(r) r^4 \rightarrow q_\infty \quad G_1(r) r^2 \rightarrow g_\infty \quad (3.26)$$

Physical quantities, namely the electric charge density ρ , the temperature T , the entropy density s , the magnetic field B_p and the 3-form charge density G_p are obtained as follows,

$$\begin{aligned} \rho &= q_\infty & T &= \frac{1}{4\pi} & B_p &= \frac{b}{v_2} \\ s &= \frac{1}{4v_1v_2} & G_p &= \frac{g_\infty}{v_1} \end{aligned} \quad (3.27)$$

In our definition of the entropy density we are absorbing Newton's constant: $s = (G_6 S)/\text{Vol}$. We also comment on the form of ρ . The electric charge of the system is given by $\int \star F$, where the integral is over a constant time slice at the boundary. Since $F = E dr \wedge dt$ we have $\star F \sim v_1 v_2 r^4 E dx^1 \wedge dx^2 \wedge dx^3 \wedge dx^4$. Dividing the integrand by $v_1 v_2$, to obtain the proper charge density, gives q_∞ . Note that the temperature in these coordinates is fixed at the constant value $T = 1/(4\pi)$. Since T is dimensionful we can always scale coordinates to bring any nonzero temperature to this value. Of course, this still allows the physically relevant dimensionless temperature (denoted below as \hat{T}) to vary.

As always, the only physically observable quantities in the conformal boundary theory are dimensionless quantities. The above physical quantities all have non-trivial scaling dimensions under $r \rightarrow \ell r$, and $x^\mu \rightarrow x^\mu/\ell$, which are given by,

$$\begin{aligned} \rho &\rightarrow \ell^4 \rho & T &\rightarrow \ell T & B_p &\rightarrow \ell^2 B_p \\ s &\rightarrow \ell^4 s & G_p &\rightarrow \ell^3 G_p \end{aligned} \quad (3.28)$$

Thus, only suitable dimensionless ratios can be physical observables. When $B_p \neq 0$, as will be almost always the case here, we may use B_b to obtain dimensionless physical observables,

$$\begin{aligned} \hat{T} &= \frac{T}{\sqrt{B_p}} = \frac{\sqrt{v_2}}{4\pi\sqrt{b}} & \hat{B} &= \frac{B_p}{\sqrt{\rho}} = \frac{b}{v_2\sqrt{q_\infty}} \\ \hat{s} &= \frac{s}{B_p^2} = \frac{v_2}{4v_1 b^2} & \hat{g} &= \frac{G_p}{\sqrt{B_p^3}} = \frac{g_\infty \sqrt{v_2^3}}{v_1 \sqrt{b^3}} \end{aligned} \quad (3.29)$$

Given that the regular supergravity solutions are completely specified by the two parameters (b, q) of the near-horizon data (whose domain is governed by regularity restrictions), together with the unique dimensionless coupling k , it follows that amongst the physical data $\hat{T}, \hat{B}, \hat{s}$, and \hat{g} , there must exist two dynamical relations, or *equations of state*. Choosing \hat{T} and \hat{B} as independent parameters (as well as k), the dynamics of the system then determines,

$$\begin{aligned}\hat{s} &= \hat{s}(k, \hat{T}, \hat{B}) \\ \hat{g} &= \hat{g}(k, \hat{T}, \hat{B})\end{aligned}\tag{3.30}$$

These functions will be obtained numerically by solving for $\hat{T}, \hat{B}, \hat{s}$, and \hat{g} in terms of the near-horizon parameters (b, q) .

4 Purely Electric and Purely Magnetic solutions

In this section, we shall briefly review the AdS_6 Reissner-Nordstrom (RN) solution for which no magnetic field is present, $B = 0$. For our purposes the RN solution is perhaps better referred to as the *purely electric solution*. We shall then exhibit an exact near-horizon solution with $B \neq 0$ but zero electric charge, whose metric is that of $\text{AdS}_4 \times \mathbf{R}^2$. The *purely magnetic solution* is the unique interpolating solution between this near-horizon solution and asymptotic AdS_6 . We shall show, numerically, that the purely magnetic solution exists and we shall characterize its asymptotics.

4.1 The purely electric solution

In the standard coordinates, the RN solution is given by,

$$U = r^2 + \frac{q^2}{6r^6} - \frac{M}{r^3} \qquad e^{2V_1} = e^{2V_2} = r^2 \qquad E = \frac{q}{r^4}\tag{4.1}$$

In the extremal limit, the location of the horizon r_+ obeys $U(r_+) = U'(r_+) = 0$, which requires the following relations between q, M and r_+ ,

$$q = \sqrt{10} r_+^4 \qquad M = \frac{8}{3} r_+^5\tag{4.2}$$

We see that the extremal entropy density s is proportional to the charge density, $s = r_+^4 \propto q$, and does not vanish as $T = 0$.

In the coordinates described in section 3.6 the RN solution is given by,

$$E = \frac{q}{(Cr + 1)^4} \qquad e^{2V_1} = e^{2V_2} = (Cr + 1)^2\tag{4.3}$$

and U takes the form,

$$U = \frac{u_0}{(Cr+1)^3} + \frac{1}{C^2}(Cr+1)^2 + \frac{q^2}{2C^2} \frac{1}{(Cr+1)^6} \quad (4.4)$$

with

$$C = \frac{10 - q^2}{2} \quad u_0 = -\frac{2 + q^2}{2C^2} \quad (4.5)$$

The extremal limit is obtained at $q^2 = 10$. The near-horizon geometry of the purely electric solution is $\text{AdS}_2 \times \mathbf{R}^4$.

4.2 The $\text{AdS}_4 \times \mathbf{R}^2$ near-horizon solution

Turning on the magnetic field modifies the near-horizon geometry. Simplest is the purely magnetic case for which the electric charge vanishes. Here, we can obtain a fairly simple picture that will be relevant for interpreting the numerics. Setting $G_1 = E = 0$, a simple solution which is regular at the horizon is then given by,

$$U = U_0 r^2 \quad e^{2V_1} = r^2 \quad e^{2V_2} = 1 \quad (4.6)$$

where the constants are given by,

$$b = \sqrt{\frac{10}{3}} \quad U_0 = \frac{20}{9} \quad (4.7)$$

This geometry is recognized as $\text{AdS}_4 \times \mathbf{R}^2$, and is the $D = 6$ analog of the $\text{AdS}_3 \times \mathbf{R}^2$ solutions studied in [13, 21]. Magnetic brane solutions have been studied further in [22, 23, 24, 25, 26], including supersymmetric examples. One lesson is that when these solutions are embedded into a higher dimensional supergravity theory they become subject to various potential instabilities, and the same could be expected of the $\text{AdS}_4 \times \mathbf{R}^2$ solution discussed here.

4.2.1 Perturbing around the $\text{AdS}_4 \times \mathbf{R}^2$ near-horizon solution

To construct solutions interpolating between $\text{AdS}_4 \times \mathbf{R}^2$ and AdS_6 we proceed by including small perturbations around $\text{AdS}_4 \times \mathbf{R}^2$ and using these to seed the flow towards AdS_6 . Since the $\text{AdS}_4 \times \mathbf{R}^2$ near-horizon solution has $E = G_1 = 0$, the linearized Einstein and gauge field equations around this solution decouple from one another.

We begin by parameterizing the small fluctuations fields for the metric as follows,

$$\begin{aligned} U(r) &= U_0 r^2 (1 + 2u(r)) \\ V_1(r) &= \frac{1}{2} \ln(U_0 r^2) + v_1(r) \\ V_2(r) &= v_2(r) \end{aligned} \quad (4.8)$$

where the fields u, v_1, v_2 are treated as first order perturbations. One obtains a closed equation for v_2 from $E3$, then an equation for v_1 from $E1$, and finally an equation for u from CON . Putting all together, we find the following system for the Einstein equations,

$$\begin{aligned} r^2 v_2'' + 4r v_2' - 9v_2 &= 0 \\ r^2 v_1'' + 2r v_1' + r^2 v_2'' &= 0 \\ 2ru' + 6u + 4r v_1' + 6r v_2' - 6v_2 &= 0 \end{aligned} \quad (4.9)$$

The equations are invariant under dilations in r , as were the original non-linear equations of (3.16), and the solutions to the linear equations are linear combinations of powers of r . For $v_2(r) \sim r^\sigma$, we must have

$$\sigma^2 + 3\sigma - 9 = 0 \quad \sigma = \frac{3}{2}(-1 + \sqrt{5}) \quad (4.10)$$

The positive root for σ has been retained here because we are after a regular perturbation near $r = 0$, requiring v_2 to vanish there. The regular solutions for the other fields are now easily found to be,

$$u(r) = v_1(r) = -\frac{\sigma - 1}{\sigma + 1} (cr)^\sigma \quad v_2(r) = (cr)^\sigma \quad (4.11)$$

Here, c is an arbitrary integration constant, or scale parameter, which may of course be absorbed into the definition of r . Equality of u and v_1 guarantees 2+1-dimensional Poincaré invariances, as expected.

Since the gauge fields of the $\text{AdS}_4 \times \mathbf{R}^2$ near-horizon solution vanish, the fields E, G_1 in the gauge field equations may be viewed themselves as parametrizing the first order fluctuations, and thus obey the linearized equations,

$$\begin{aligned} (U_0 r^2 E)' + kb G_1 &= 0 \\ G_1' + 2kb E &= 0 \end{aligned} \quad (4.12)$$

where the constants b and U_0 are given by (4.7). Eliminating G_1 , we find the following equation $(r^2 E)'' - 6k^2 E = 0$ for E . This is, of course, again scale invariant, so that its solutions are linear combinations of powers of r . The full solution is found to be given by,

$$E(r) = r^\kappa \quad G_1(r) = -\frac{(\kappa + 2)b}{3k} r^{\kappa+1} \quad (4.13)$$

where the exponent κ must satisfy,

$$(\kappa + 2)(\kappa + 1) - 6k^2 = 0 \quad \kappa = -\frac{3}{2} + \frac{1}{2}\sqrt{1 + 24k^2} \quad (4.14)$$

The positive square root chosen above is dictated by the regularity at the horizon of the gauge potential A , which is defined by $E = A'$ together with its vanishing at the horizon. Note that we then have $\kappa \geq -1$ for all k , with equality only for $k = 0$. The electric field itself is regular at the horizon provided $\kappa \geq 0$, namely when

$$k \geq k_c = \frac{1}{\sqrt{3}} \quad (4.15)$$

This condition singles out the value k_c for the coupling k (which will turn out to be a *critical value*) as a rough analogue of the special value $k = 1$ for the AdS_5 case [8].

4.3 The purely magnetic brane solution

We have not succeeded in solving analytically the reduced Einstein equations for the purely magnetic brane (the gauge field equations of (3.19) are satisfied automatically for zero charge when $E = G_1 = 0$). Numerical analysis is, however, straightforward and shows that the first order perturbation of the metric around the $\text{AdS}_4 \times \mathbf{R}^2$ near-horizon solution, computed in section 4.2.1, extends into a full fledged solution of the non-linear equations which interpolates to asymptotically AdS_6 . Given the above normalizations at the horizon, the AdS_6 data result as follows,

$$\frac{U(r)}{r^2} \rightarrow 1 \quad \frac{e^{2V_1(r)}}{r^2} \rightarrow 1 \quad \frac{e^{V_2(r)}}{r^2} = C_v \quad (4.16)$$

and C_v is obtained numerically, and given by $C_v = 1.221905$.

4.4 Entropy density of purely magnetic brane for small T^2/B

In the purely magnetic case an expression for the low temperature entropy density may be obtained analytically, as we now discuss. This provides a useful check on the numerics.

The purely magnetic brane solution takes the form,

$$\begin{aligned} ds^2 &= \frac{dr^2}{U} - U dt^2 + e^{2V_1} \left((dx^1)^2 + (dx^2)^2 \right) + e^{2V_2} \left((dx^3)^2 + (dx^4)^2 \right) \\ F &= B dx^3 \wedge dx^4 \end{aligned} \quad (4.17)$$

At zero temperature we have Lorentz invariance in (t, x^1, x^2) , and this fixes $e^{2V_1} = U$. The zero temperature solution has near-horizon geometry $\text{AdS}_4 \times \mathbf{R}^2$, so that, as $r \rightarrow 0$,

$$U = U_0 r^2 \quad e^{2V_2} = \sqrt{\frac{3}{10}} B \quad (4.18)$$

with $U_0 = 20/9$, as was given in (4.7).

At small but finite temperature the near-horizon AdS₄ is replaced by the near-horizon AdS₄ Schwarzschild solution, given by,

$$U = U_0 \left(r^2 - \frac{r_+^3}{r} \right) \quad e^{2V_1} = U_0 r^2 \quad e^{2V_2} = \sqrt{\frac{3}{10}} B \quad (4.19)$$

This is valid provided the horizon lies well within the AdS₄ region, namely for $r_+ \ll 1$. This translates into the condition $T^2/B \ll 1$. The entropy density and temperature are

$$G_6 S = \frac{A_H}{4} = \frac{1}{4} \sqrt{\frac{3}{10}} U_0 B r_+^2 V_4 \quad T = \frac{U'(r_+)}{4\pi} = \frac{3U_0 r_+}{4\pi} \quad (4.20)$$

where V_4 is the coordinate volume. Eliminating r_+ between these expressions, we compute the entropy density s as a function of temperature,

$$s = \frac{G_6 S}{V_4} = \sqrt{\frac{3}{10}} \frac{\pi^2}{5} B T^2 \approx 1.08 B T^2 \quad (4.21)$$

The T^2 dependence is characteristic of a $2 + 1$ dimensional CFT; this CFT is associated to the near-horizon AdS₄ region.

5 Lifshitz solutions for critical k

The near-horizon Reissner-Nordstrom black brane geometry for $k < k_c$, and the near-horizon AdS₄ \times \mathbf{R}^2 for $k > k_c$ are separated by a Lifshitz near-horizon geometry for $k = k_c$. The fields for the corresponding near-horizon solution will be computed analytically in this section. Linearized fluctuations around this solution smoothly connect onto solutions to the full fledged non-linear reduced field equations which interpolate to AdS₆, as will be shown in this section, using the results of Appendix A.

5.1 Near horizon Lifshitz solution

In this sub-section we look for scale invariant solutions that can play the role of near-horizon geometries in the presence of nonzero electric charge and magnetic field. We start from the Ansatz arrived at in section 3.5 for the metric,

$$ds^2 = \frac{dr^2}{U} - U dt^2 + e^{2V_1} \left((dx^1)^2 + (dx^2)^2 \right) + e^{2V_2} \left((dx^3)^2 + (dx^4)^2 \right) \quad (5.1)$$

and for the gauge fields,

$$\begin{aligned} F &= E(r) dr \wedge dt + b_0 dx^3 \wedge dx^4 \\ G &= G_1(r) dr \wedge dx^1 \wedge dx^2 \end{aligned} \quad (5.2)$$

We look for a solution which is invariant under scale transformations of the form,

$$r \rightarrow \lambda r \quad t \rightarrow \frac{1}{\lambda} t \quad x^{1,2} \rightarrow \frac{1}{\lambda^\alpha} x^{1,2} \quad x^{3,4} \rightarrow \frac{1}{\lambda^\beta} x^{3,4} \quad (5.3)$$

for some real constants α and β . Scale invariance requires,

$$U = u_0 r^2 \quad e^{2V_1} = r^{2\alpha} \quad e^{2V_2} = r^{2\beta} \quad E = q_0 \quad G_1 = g_1 r^{2\alpha-1} \quad (5.4)$$

where we used the freedom to rescale x^i to fix the prefactors of $e^{2V_{1,2}}$. The metric is of the Lifshitz type [19]. We now substitute these expressions into the reduced field equations written in section 3.5.

Assuming $b_0 \neq 0$, equation $E2$ implies $\beta = 0$, since all terms in $E2$ are constant except for the final term, which behaves as $b_0^2 r^{-4\beta}$. Solving $M1$ and $M2$ requires,

$$u_0 = \frac{2k^2 b_0^2}{\alpha} \quad g_1 = -\frac{q_0 \alpha}{k b_0} \quad (5.5)$$

Solving $E1$ gives,

$$q_0^2 = \left(\frac{1-\alpha}{\alpha} \right) k^2 b_0^2 \quad (5.6)$$

We then find,

$$E2 - E3 = 2b_0^2(3k^2 - 1) \quad (5.7)$$

which, assuming as always $b_0 \neq 0$, forces,

$$k = k_c = \frac{1}{\sqrt{3}} \quad (5.8)$$

The remaining equations reduce to the following quadratic equation for α ,

$$\left(\alpha + \frac{1}{2} \right)^2 = \frac{15}{2b_0^2} \alpha \quad (5.9)$$

Its solutions may be parameterized as follows,

$$q_0^2 = \frac{10z(z-1)}{(z+2)^2} \quad b_0^2 = \frac{30z}{(z+2)^2} \quad (5.10)$$

where we have defined,

$$z = \frac{1}{\alpha} \quad (5.11)$$

From (5.3) we see that z is the dynamical critical exponent, since under scaling $t \sim (x^{1,2})^z$.

We have therefore found a one parameter family of solutions $\text{Lif}_4 \times \mathbf{R}^2$ parameterized by the dynamical exponent z . From (5.10) it is clear that we should restrict to $z \geq 1$ in order that q_0 and b_0 be real. All values $z \geq 1$ are allowed. For $z = 1$ we recover the purely magnetic $\text{AdS}_4 \times \mathbf{R}^2$ solution, with $(b_0, q_0) = (\sqrt{10/3}, 0)$. As $z \rightarrow \infty$ we go over to the purely electric $\text{AdS}_2 \times \mathbf{R}^4$ solution with $(b_0, q_0) = (0, \sqrt{10})$. For $k \neq k_c$, only the purely magnetic/electric solutions exist.

5.2 Interpolating solution

We now look for solutions that interpolate between these $k = k_c$ near-horizon solutions and an asymptotic AdS_6 . Here we proceed numerically. We first solve for linearized fluctuations around $\text{Lif}_4 \times \mathbf{R}^2$, identify those that are nonsingular in the near-horizon region, and then use these as seeds for the numerical integration out to large r . The details are described in Appendix A. The upshot is that we find smooth asymptotically AdS_6 solutions for the full family of near-horizon solutions described above.

6 Flows towards low temperature

We now study the thermodynamics of solutions with nonzero charge and magnetic field. In the high temperature limit the behavior is universal, and is governed by the AdS_6 Schwarzschild black brane. The entropy density behaves as $s \propto T^4$, as appropriate for a 4+1 dimensional CFT. The low temperature behavior is much more interesting, as it is sensitive to the charge density, magnetic field, and Chern-Simons coupling k . We have already identified $k_c = 1/\sqrt{3}$ as the critical value of k for which a near-horizon Lifshitz geometry arises, and so we can expect a qualitative change in behavior depending on the size of k relative to k_c , as was summarized in the Introduction. Here we supply more of the details.

The discussion in sections 3.6 and 3.7 provides the basis for our numerical evaluation of the entropy density. As described there, after fixing coordinates the near-horizon data is parameterized by specifying the pair (b, q) , representing the near-horizon electric and magnetic fields. Numerical integration outwards in r for each choice of (b, q) (and for a given k) yields either a smooth asymptotically AdS_6 solution or a singularity. We discard the singular solutions, which requires that we restrict attention to a finite region in the (b, q) plane. For each (b, q) within the allowed region we compute the dimensionless quantities $(\hat{T}, \hat{s}, \hat{B}, \hat{g})$ from the asymptotic data at the AdS_6 boundary. Our main interest is in understanding the behavior of $\hat{s}(\hat{T})$ at fixed \hat{B} . As we have noted, this depends crucially on the size of k relative to k_c , and we discuss the three cases in turn.

6.1 Low temperature thermodynamics: $k > k_c$

At vanishing charge density, corresponding to $\hat{B} \rightarrow \infty$, the low temperature entropy density was found analytically in (4.21). In terms of dimensionless quantities the result is,

$$\hat{s} = \sqrt{\frac{3}{10}} \frac{\pi^2}{5} \hat{T}^2 \quad \text{as } \hat{T} \rightarrow 0 \quad \text{at } \hat{B} = \infty \quad (6.1)$$

More generally, at finite \hat{B} the numerics show the low temperature behavior, as $\hat{T} \rightarrow 0$,

$$\hat{s} = A(k, \hat{B}) \hat{T}^2 \quad (6.2)$$

Typical examples are shown in figure 4.

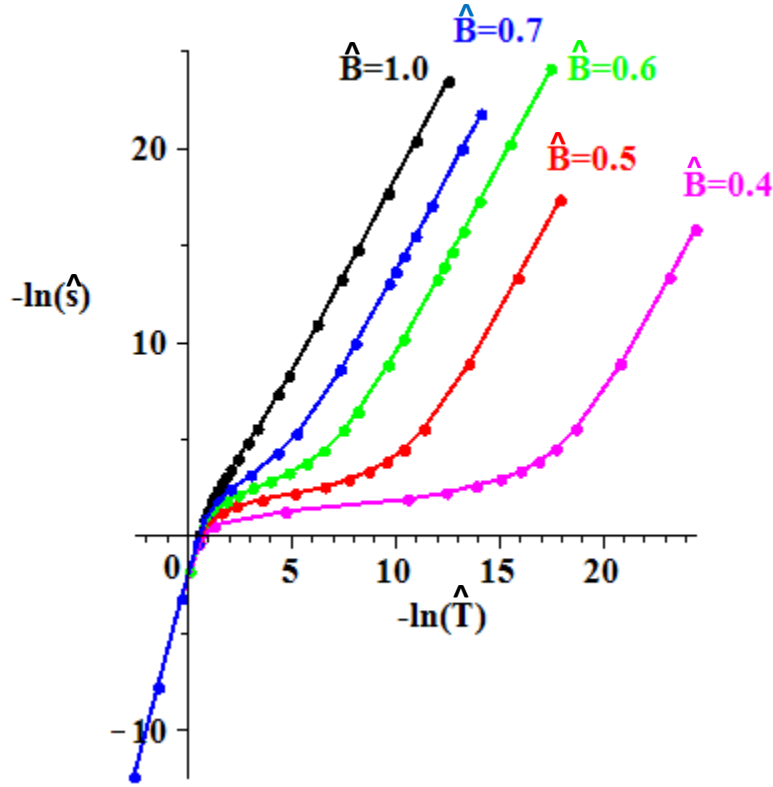


Figure 4: Entropy density versus temperature at $k = 0.7$ for selected values of \hat{B} .

The \hat{T}^2 dependence of the entropy density is associated with a near-horizon $\text{AdS}_4 \times \mathbf{R}^2$ geometry, in particular the one discussed in section 4.2. We note that the electric field

vanishes in the near-horizon region, $E = 0$, which makes it clear that the electric flux measured at the AdS_6 boundary is sourced by fields living outside the near-horizon region. As emphasized in the Introduction, it is the modification of Gauss' law brought about by the Chern-Simons term that allows the combined magnetic field and three form field strength to act as a charge density. For $k > k_c$, we see that all of the charge density measured at the AdS_6 boundary is generated by this mechanism.

Another way to exhibit the appearance of $\text{AdS}_4 \times \mathbf{R}^2$ is to plot the flow in (b, q) space as we lower the temperature, as shown in figure 2. Lowering the temperature at fixed \hat{B} , we find that we are driven to the point $(b = \sqrt{10/3}, q = 0)$. This point represents the pure magnetic brane solution; of course, we never reach precisely this point, since we are keeping \hat{B} fixed at a finite value, while the magnetic brane has $\hat{B} = \infty$.

Next we consider decreasing \hat{B} . Strictly at $\hat{B} = 0$, we know that we should recover the pure electric RN solution and its nonzero ground state entropy density, and so it is clear that $A(k, \hat{B})$ must be singular at $\hat{B} = 0$. The numerics show the following behavior as $\hat{B} \rightarrow 0$,

$$A(k, \hat{B}) \sim c(k) \exp \left\{ \frac{d(k)}{\hat{B}^2} \right\} \quad (6.3)$$

for some k -dependent real positive constants c and d ; see figure 5. On general grounds we expect that this singularity structure should be amenable to analytical understanding, but this is lacking at present.

6.2 Low temperature thermodynamics: $k < k_c$

For sufficiently small k the effect of the Chern-Simons term is too weak to allow for all the charge density to be carried by flux. Some fraction of the flux is instead hidden behind an event horizon, and associated with this horizon is a nonzero ground state entropy density. Indeed, for $k < k_c$ there appears to be such an entropy for any finite \hat{B} . Representative numerical results are shown in figure 2. Note that increasing \hat{B} suppresses the value of the extremal entropy.

The near-horizon geometry obtained at $\hat{T} = 0$ in this regime is $\text{AdS}_2 \times \mathbf{R}^4$. This can also be seen by studying the flow in (b, q) space. As \hat{T} is lowered at fixed \hat{B} , we flow towards $(b = 0, q = \sqrt{10})$, which is the pure electric fixed point. This is illustrated in Figure 2.

Increasing k at fixed \hat{B} again reveals k_c to represent a critical value. In particular, the extremal entropy tends toward zero as k approaches k_c from below; this behavior can be seen in figure 2.

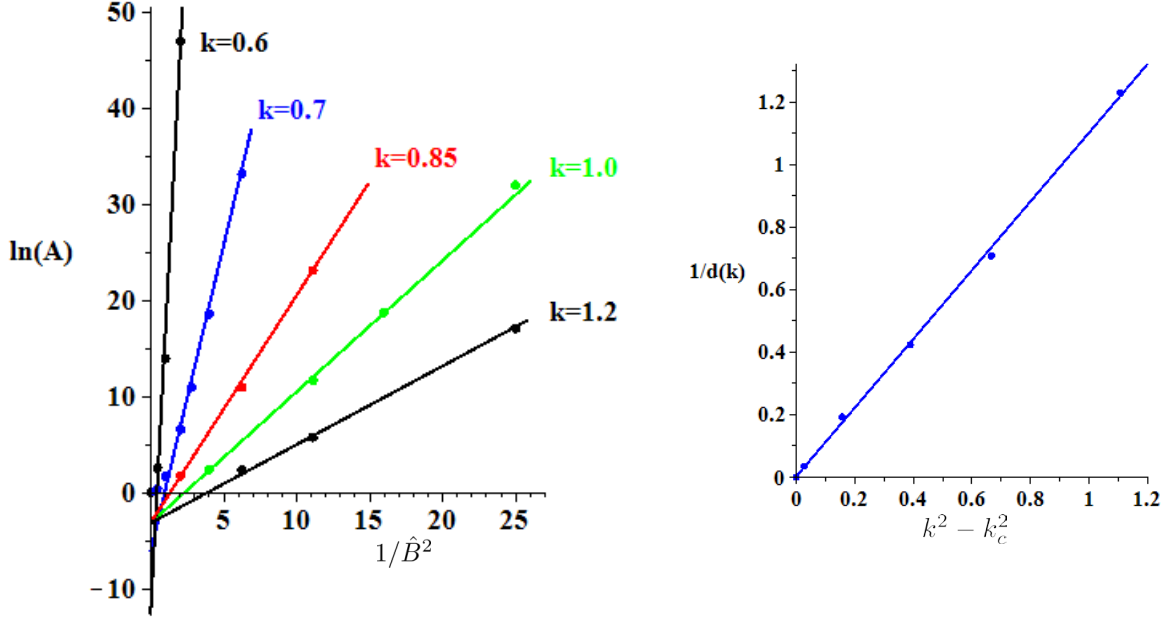


Figure 5: Data illustrating the divergence of $A(k, \hat{B})$ as $\hat{B} \rightarrow 0$, in accord with (6.3).

6.3 Low temperature thermodynamics: $k = k_c$

At the critical value of k , taking the temperature to zero reveals the appearance of the near-horizon $\text{Lif}_4 \times \mathbf{R}^2$ geometry discussed in section 5. Examining the flow in (b, q) space as in figure 2 shows that, rather than flowing to either the pure electric or pure magnetic fixed point, the IR flow is towards a point on a critical curve. To explain this we first note that according to (5.10) the parameters of the $\hat{T} = 0$ $\text{Lif}_4 \times \mathbf{R}^2$ solution obey,

$$3(q_0^2 + b_0^2)^2 - 10(b_0^2 + 3q_0^2) = 0 \quad (6.4)$$

This same curve governs the $\hat{T} \rightarrow 0$ behavior of possible values of (b, q) , up to the fact that there is a finite renormalization relating (b, q) to (b_0, q_0) . This renormalization comes about from the fact that (b, q) are defined at the horizon of a finite temperature solution in a coordinate system (defined in section 3.6) that does not agree, in the zero temperature limit, with that used to write the zero temperature solution in which (b_0, q_0) appear. The coordinate transformation that relates the two solution induces a change in the parameters. However, as the temperature is taken to zero, the two coordinate systems differ only in a shrinking region near the horizon and, as long as one stays outside this region, the parameters (b_0, q_0) can be read off from the finite temperature solution, and the critical curve (6.4) is reproduced from the numerics. This procedure is explained in more detail Appendix B.

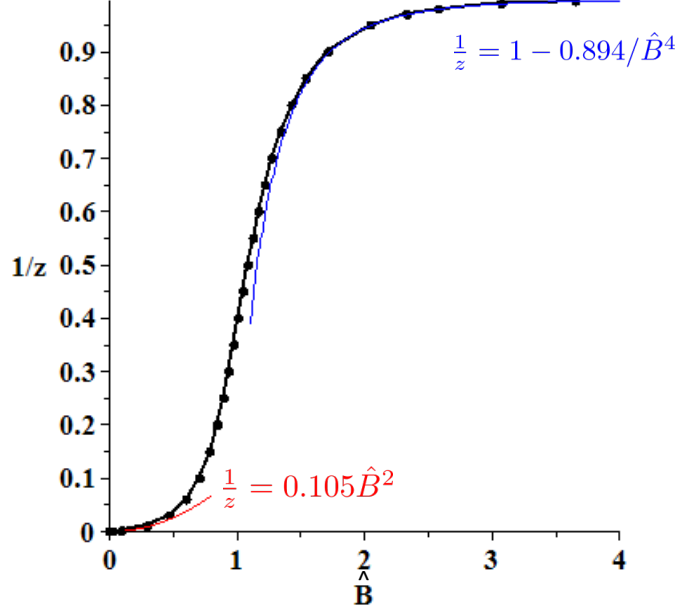


Figure 6: Dynamical critical exponent $z = 1/\alpha$ as a function of \hat{B} for $k = k_c$.

The critical curve can be parameterized by the dynamical exponent z , according to (5.10). The critical curve connects the electric fixed point at $b = 0$ and the magnetic fixed point at $q = 0$. The full curve is traversed as \hat{B} ranges from 0 to ∞ . There is thus a relation between the dynamical exponent z and the magnetic field, $z = z(\hat{B})$. However, the precise form of this relation depends on the full interpolating solution connecting the near-horizon region to AdS_6 . This is because \hat{B} is defined in terms of asymptotic data, while (b, q) are near-horizon data. Numerically, we find that $z(\hat{B})$ takes the form shown in figure 6.

The low temperature entropy takes a form dictated by the near-horizon Lifshitz symmetry, namely, as $\hat{T} \rightarrow 0$ we have,

$$\hat{s} = f(\hat{B}) \hat{T}^{2/z} \quad z = z(\hat{B}) \quad (6.5)$$

We have not attempted to characterize the prefactor $f(\hat{B})$, but it presumably depends on the full interpolating solution.

These solutions also carry a nonzero value for the three-form charge \hat{g} . Its behavior is shown in figure 7. The power law dependence for large and small \hat{B} can be understood as follows. First consider the $\hat{B} \rightarrow 0$ behavior. At $B = 0$ we have the purely electric RN solution, which has $G = 0$. We can use perturbation theory around the purely electric solution to add in a small B . Assuming a finite radius of convergence, we expect that the leading behavior of G_p is linear in B_p , where we now refer to the physical quantities

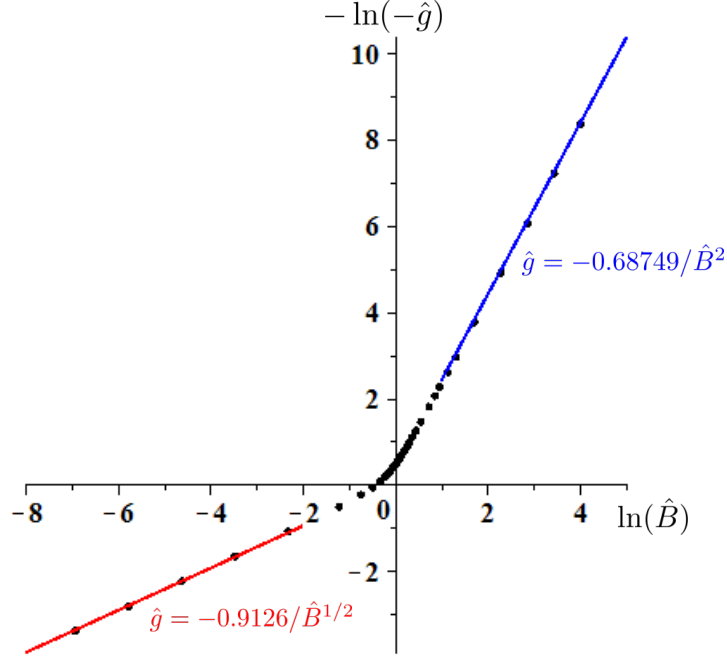


Figure 7: Plot of the three-form charge \hat{g} as a function of \hat{B} at $T = 0$ and $k = k_c$.

defined in (3.27). The ρ dependence is then fixed by the scale transformations defined in (3.28), which give $G_p \sim \rho^{1/4} B_p$. Converting to hatted quantities, this is $\hat{g} \sim 1/\hat{B}^{1/2}$, which agrees with the behavior in figure 7. The same type of argument holds for $\hat{B} \rightarrow \infty$, now involving perturbation theory around the purely magnetic solution. The fact that the numerics agree with these arguments based on perturbation theory can be taken as evidence that perturbation theory is convergent.

7 Quantum critical behavior

Our analysis has revealed two interesting examples of quantum critical behavior in this system, as manifested by the low temperature thermodynamics. In particular, we focus on non-analytic behavior in terms of the control parameters k and \hat{B} , and the temperature \hat{T} .

In the regime $k > k_c$ we found nonanalytic behavior at $\hat{B} = 0$. This is associated with the fact that an infinitesimally small magnetic field is enough to remove the ground state entropy density of the pure electric RN black brane. Quantitatively, we saw nonanalytic behavior in the coefficient of the \hat{T}^2 term in the entropy density as $\hat{B} \rightarrow 0$. As noted already, we lack a good analytical understanding of this critical behavior.

A second example of quantum criticality was found at $k = k_c$, and governed by the appearance of a near-horizon Lifshitz geometry. We explored the approach to this critical point from several directions, either by decreasing \hat{T} at fixed \hat{B} and k , and by letting k approach k_c at fixed \hat{B} and (low) \hat{T} . More generally, there will exist a full scaling form for the entropy density in the vicinity of the critical point

$$\hat{s} = F(k - k_c, \hat{B}, \hat{T}) \quad (7.1)$$

In the analogous AdS₅ critical point the full scaling function was computed analytically in [8], and it would of course be interesting to achieve that for the present case as well, but we leave that for the future.

The two control parameters k and \hat{B} are on somewhat different footings in the (nominal) dual CFT. \hat{B} is built out of the magnetic field B and charge density ρ . Changing ρ corresponds to considering a different state of the CFT, while changing B is accomplished by varying an external field. On the other hand, we expect that to change k we need to change the field content of the CFT. Chern-Simons terms in the bulk are related to anomalies in the dual CFT, and these are determined by the field content. It is therefore unclear whether we could ever realize the precise value k_c , or whether it is physically sensible to think about tuning k . On the other hand, the familiar “fanlike” structure governing finite temperature behavior near a quantum critical point shows that it is not necessary to sit precisely at the critical point in order to detect its influence.

The critical D=2+1 theories studied here violate parity due to the three-form field strength $G = G_1 dr \wedge dx^1 \wedge dx^2$. In the boundary CFT, this corresponds to an expectation value of some two-form operator, $\langle \mathcal{O}_{12} \rangle = -\langle \mathcal{O}_{21} \rangle$. Since we haven’t proposed a specific CFT dual, we of course cannot say what this operator is. But given such a dual CFT, we expect that this two-form operator will play an important role in driving the quantum phase transition.

Acknowledgments

We thank Eric Perlmutter for discussions. Eric D’Hoker wishes to thank the Laboratoire de Physique Théorique del’Ecole Normale Supérieure, and the Laboratoire de Physique Théorique et Hautes Energies, CNRS and Université Pierre et Marie Curie - Paris 6, and especially Constantin Bachas and Jean-Bernard Zuber for their warm hospitality while part of this work was being completed.

A Linearization around near-horizon Lifshitz

The near-horizon Lifshitz geometry present for $k = k_c$ smoothly extends into a solution of the full non-linear reduced field equations which is asymptotic to AdS₆ for large r . To

date, these full non-linear equations have not been solved analytically, but the numerical evidence for their existence is overwhelming. The numerical solution is obtained by solving the full non-linear reduced equations starting from the near-horizon Lifshitz solution plus first order perturbative corrections around Lifshitz. As is familiar from the study of the purely magnetic brane in AdS_5 , the first order fluctuations, subject to appropriate near-horizon boundary conditions, will act as seeds for the full non-linear solution with the same boundary conditions.

In this Appendix, we shall compute the first order fluctuations around the Lifshitz solution for $k = k_c$. To set up the problem, it is preferable to use the parameter $\alpha = z^{-1}$ instead of the dynamical scaling exponent z . In terms of α , the data of the Lifshitz solution may be expressed as follows,

$$\begin{aligned} U(r) &= u_0 r^2 & E(r) &= q_0 \\ V_1(r) &= \alpha \ln(r) & G(r) &= g_0 r^{2\alpha-1} \\ V_2(r) &= 0 \end{aligned} \tag{A.1}$$

Here, u_0, q_0, g_0 , and α are constants related to k and the value b_0 of the field B near the horizon with the normalization $V_2(0) = 0$. The values of the remaining constants may be conveniently parameterized in terms of α ,

$$\begin{aligned} b_0 &= \frac{\sqrt{30\alpha}}{2\alpha+1} & q_0 &= \frac{\sqrt{10(1-\alpha)}}{2\alpha+1} \\ u_0 &= \frac{20}{(2\alpha+1)^2} & g_0 &= -\sqrt{\alpha(1-\alpha)} \end{aligned} \tag{A.2}$$

Reality of b_0, q_0 and g_0 clearly requires that α be restricted to the range,

$$0 \leq \alpha \leq 1 \tag{A.3}$$

This condition restricts b_0^2 to the interval $0 \leq b_0^2 \leq 15/4$, the upper value being attained when $\alpha = 1/2$. It also restricts q_0^2 to the interval $0 \leq q_0^2 \leq 10$, the upper value corresponding to the Reissner-Nordstrom black brane. Recall that the critical curve in terms of near-horizon data (b_0, q_0) is obtained by eliminating α from the above relations, and takes the form,

$$3(b_0^2 + q_0^2)^2 - 10(b_0^2 + 3q_0^2) = 0 \tag{A.4}$$

A.1 Linearized reduced field equations

The linearization problem is parameterized as follows,

$$U(r) = u_0 r^2 + u_1(r)$$

$$\begin{aligned}
V_1(r) &= \alpha \ln(r) + v_1(r) \\
V_2(r) &= v_2(r) \\
E(r) &= q_0(1 + e_1(r)) \\
G(r) &= g_0 r^{2\alpha-1} \left(1 + \frac{1}{\alpha} g_1(r)\right)
\end{aligned} \tag{A.5}$$

Here the fluctuation fields u_1, v_1, v_2, e_1 , and g_1 are treated as first order quantities, higher orders therein being neglected in the range where all these fields are small. The precise normalization of e_1 and g_1 has been introduced for later convenience.

The corresponding linearized reduced Einstein field equations are given by,

$$\begin{aligned}
E1 \quad 0 &= r^2 v_1'' + r^2 v_2'' + 2\alpha r v_1' - 4\alpha(1 - \alpha)v_1 - 2(1 - \alpha)g_1 \\
E2 \quad 0 &= 20r^2 v_1'' + 40(2\alpha + 1)rv_1' + 40\alpha r v_2' + \alpha(2\alpha + 1)^2 r u_1' - 80\alpha(1 - \alpha)v_1 \\
&\quad + 60\alpha v_2 + (4\alpha^4 + 12\alpha^3 + 9\alpha^2 + 2\alpha)u_1 + 10(1 - \alpha)e_1 - 40(1 - \alpha)g_1 \\
E3 \quad 0 &= 20r^2 v_2'' + 40(1 + \alpha)rv_2' + 80\alpha(1 - \alpha)v_1 - 180\alpha v_2 \\
&\quad + (4\alpha^4 - 3\alpha^2 - \alpha)u_1 + 40(1 - \alpha)g_1 + 10(1 - \alpha)e_1 \\
E4 \quad 0 &= (2\alpha + 1)^2 r^2 u_1'' + (8\alpha^3 + 24\alpha^2 + 18\alpha + 4)ru_1' \\
&\quad + 80r(v_1' + v_2') + (8\alpha^4 + 16\alpha^3 + 18\alpha^2 + 10\alpha + 2)u_1 \\
&\quad + 160\alpha(1 - \alpha)v_1 + 120\alpha v_2 - 60(1 - \alpha)e_1 + 80(1 - \alpha)g_1
\end{aligned} \tag{A.6}$$

The reduced Maxwell-two-form equations are given by,

$$\begin{aligned}
M1 \quad 0 &= r e_1' + 2r(v_1' + v_2') + 4\alpha(v_1 + v_2) + 2\alpha e_1 + 2g_1 \\
M2 \quad 0 &= 20r g_1' - \alpha(2\alpha + 1)^2 u_1' + 40\alpha r(v_1' - v_2') \\
&\quad - (4\alpha^3 + 4\alpha^2 + \alpha)u_1 + 40\alpha(v_1 - v_2) + 20\alpha e_1 + 20g_1
\end{aligned} \tag{A.7}$$

There is also the constraint,

$$\begin{aligned}
CON \quad 0 &= \alpha(2\alpha + 1)^2 r u_1' + 40(1 + \alpha)rv_1' + 40(2\alpha + 1)rv_2' \\
&\quad + (8\alpha^4 + 12\alpha^3 + 6\alpha^2 + \alpha)u_1 + 80\alpha(1 - \alpha)v_1 - 120\alpha v_2 \\
&\quad + 20(1 - \alpha)e_1 + 40(1 - \alpha)g_1
\end{aligned} \tag{A.8}$$

whose r -derivative is a linear combination of $E1, E2, E3, E4, M1$, and $M2$.

A.2 Solution to the linearized equations

As a result of the scale invariance of the Lifshitz background solution, the linearized equations are invariant under an arbitrary rescaling of r . This is manifest also from the observation that

the equations above are linear differential equations with constant coefficients with respect to the differential operator $r d/dr$. Thus, the system may be solved by a linear superposition of powers of r . Concretely, we set

$$\begin{pmatrix} v_1(r) \\ v_2(r) \\ u_1(r) \\ e_1(r) \\ g_1(r) \end{pmatrix} = r^\lambda \mathcal{V} \quad \mathcal{V} = \begin{pmatrix} \mathcal{V}_1 \\ \mathcal{V}_2 \\ \mathcal{U}_1 \\ \mathcal{E}_1 \\ \mathcal{G}_1 \end{pmatrix} \quad (\text{A.9})$$

where $\mathcal{V}_1, \mathcal{V}_2, \mathcal{U}_1, \mathcal{E}_1, \mathcal{G}_1$ are independent of r . The allowed values of the exponent λ are to be determined by substituting (A.9) into equations (A.6), (A.7) and (A.8). The resulting equation may be recast in the form $\mathcal{A}\mathcal{V} = 0$. The explicit form of \mathcal{A} may be deduced from (A.6), (A.7) and (A.8), but will not be written out here. Using Maple, one computes,

$$\det \mathcal{A} = 400\alpha(2\alpha + 1)^2 l^2 (l + 1)(l + 2\alpha + 1)^2 (l^2 + (2\alpha + 1)l - 6\alpha^2 - \alpha - 2) \quad (\text{A.10})$$

For the double zeros of the determinant, at $\lambda = 0$ and at $\lambda = -1 - 2\alpha$, the general solution is obtained by replacing $r^\lambda \mathcal{V}$ in (A.9) by $r^\lambda \mathcal{V} + r^\lambda \ln(r) \tilde{\mathcal{V}}$. Here, $\tilde{\mathcal{V}}$ and \mathcal{V} obey the relations $\mathcal{A}\tilde{\mathcal{V}} = 0$ and $\mathcal{A}\mathcal{V} + \mathcal{B}\tilde{\mathcal{V}} = 0$, and we shall not need the explicit form of \mathcal{B} .

The modes corresponding to $\lambda = 0$ and $\lambda = -1$ respectively correspond to the dilation zero mode of the Lifshitz background, and to its translation mode. The dilation modes are non-vanishing at the horizon, therefore modify the horizon data, and are thus excluded from contributing. The $\lambda = -1$ and $\lambda = -1 - 2\alpha$ modes are both singular at the horizon, and cannot contribute either. This leaves the modes for which λ obeys,

$$l^2 + (2\alpha + 1)l - 6\alpha^2 - \alpha - 2 = 0 \quad (\text{A.11})$$

This equation is solved as follows,

$$\lambda_\pm = -\alpha - \frac{1}{2} \pm \Delta \quad \Delta = \frac{1}{2} \sqrt{28\alpha^2 + 8\alpha + 9} \quad (\text{A.12})$$

In the interval $0 \leq \alpha \leq 1$, only the branch l_+ is regular, since we have $l_- < -2$, and $l_+ > 1/2$. Thus, only the branch l_+ needs to be retained for matching. The corresponding eigenvector is given by the following components,

$$\begin{aligned} \mathcal{V}_1 &= -\mathcal{J}(456\alpha^5 + 164\alpha^4 + 78\alpha^3 - 185\alpha^2 - 64\alpha - 44) \\ \mathcal{V}_2 &= \mathcal{J}(192\alpha^5 + 376\alpha^4 + 128\alpha^3 + 106\alpha^2 + 8) + \Delta \mathcal{J}(12\alpha^4 - 8\alpha^3 + 49\alpha^2 + 16\alpha + 12) \\ \mathcal{U}_1 &= \frac{40\mathcal{J}}{\alpha(2\alpha + 1)^2} \left(192\alpha^6 - 560\alpha^5 + 84\alpha^4 - 188\alpha^3 + 75\alpha^2 - 20\alpha + 12 \right. \\ &\quad \left. + \Delta \{ 12\alpha^5 + 76\alpha^4 - 47\alpha^3 - 21\alpha^2 - 16\alpha - 4 \} \right) \end{aligned}$$

$$\begin{aligned}
\mathcal{E}_1 &= \frac{4\mathcal{J}}{2\alpha+1} \left(216\alpha^5 - 324\alpha^4 - 70\alpha^3 - 183\alpha^2 - 24\alpha - 20 \right. \\
&\quad \left. + 2\Delta\{-36\alpha^4 + 12\alpha^3 - 17\alpha^2 - 4\} \right) \\
\mathcal{G}_1 &= 2\mathcal{J} \left(840\alpha^6 + 244\alpha^5 + 286\alpha^4 - 149\alpha^3 + 12\alpha^2 - 30\alpha + 12 \right) \\
&\quad + 4\Delta J \left(12\alpha^5 + 28\alpha^4 + 21\alpha^3 + 3\alpha^2 + \alpha - 2 \right)
\end{aligned} \tag{A.13}$$

where \mathcal{J} is the overall normalization of the eigenvector.

Maple calculations, using the above regular branch of the perturbative solution as initial conditions, clearly demonstrate that the perturbative solution continues into a regular asymptotically AdS₆ solution.

B Identification of (b_0, q_0) in low \hat{T} solutions at $k = k_c$

Numerical solutions, obtained with initial conditions at the horizon at finite temperature, are governed by the data q and b at the horizon, as defined in the coordinate system employed in the numerics. These parameters do not coincide exactly with the parameters q_0 and b_0 of the $\hat{T} = 0$ solutions because a finite renormalization effect from finite \hat{T} boundary conditions to the $\hat{T} = 0$ scaling solution takes place. This effect is illustrated in the left panel of figure 8. At very low \hat{T} , the functions $e^{2V_2(r)}$ and $E(r)$ settle to a value which is constant over a large number of e -folds, and to high precision. It is the values of $e^{2V_2(r)}$ and $E(r)$ in this regime that determine b_0 and q_0 in terms of b and q .

The corresponding assignments for q_0 and b_0 , derived from the numerical runs at finite but very low \hat{T} , may be plotted and compared with the critical curve which is given exactly by A.4. The corresponding plot is given in the right panel of figure 8, showing excellent agreement throughout the curve.

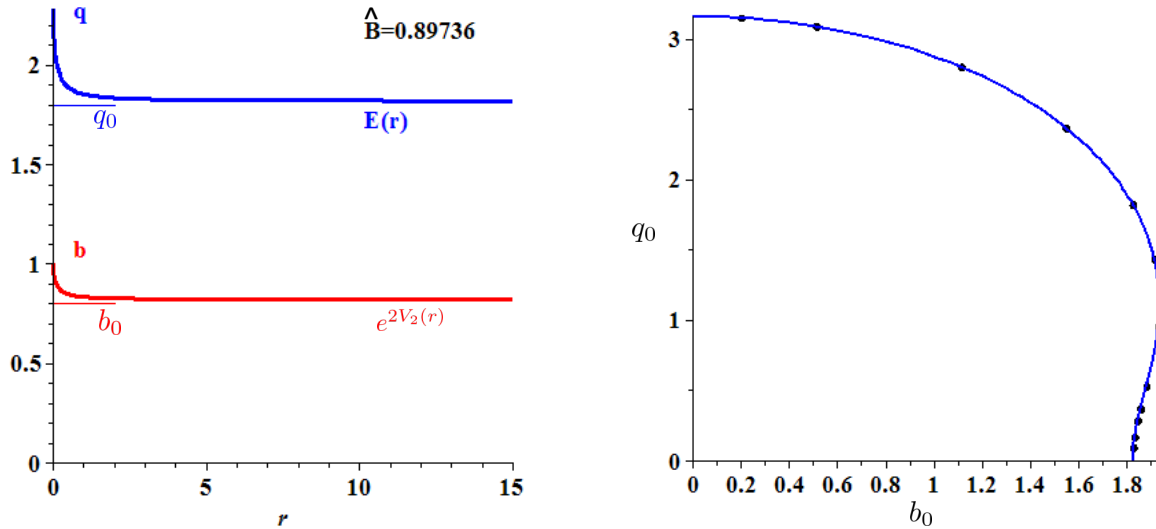


Figure 8: Left panel: finite renormalization effects occur in transitioning between the finite \hat{T} initial data (b, q) at the horizon, and the initial data (b_0, q_0) at the horizon of the scaling solution. Right panel: the blue line represents the critical curve $3(b_0^2 + e_0^2)^2 = 10b_0^2 + 30e_0^2$; the data point were collected in the scaling region from the low \hat{T} numerical solutions.

References

- [1] S. A. Hartnoll, “Lectures on holographic methods for condensed matter physics,” Class. Quant. Grav. **26**, 224002 (2009) [arXiv:0903.3246 [hep-th]].
- [2] C. P. Herzog, “Lectures on Holographic Superfluidity and Superconductivity,” J. Phys. A A **42**, 343001 (2009) [arXiv:0904.1975 [hep-th]].
- [3] S. Sachdev, “Quantum Phase Transitions”, Cambridge University Press, 2011
- [4] S. Sachdev, “Holographic metals and the fractionalized Fermi liquid,” Phys. Rev. Lett. **105**, 151602 (2010) [arXiv:1006.3794 [hep-th]].
- [5] S. A. Hartnoll, C. P. Herzog and G. T. Horowitz, “Building a Holographic Superconductor,” Phys. Rev. Lett. **101**, 031601 (2008) [arXiv:0803.3295 [hep-th]].
- [6] S. A. Hartnoll and A. Tavanfar, “Electron stars for holographic metallic criticality,” Phys. Rev. D **83**, 046003 (2011) [arXiv:1008.2828 [hep-th]].
- [7] E. D’Hoker and P. Kraus, “Holographic Metamagnetism, Quantum Criticality, and Crossover Behavior,” JHEP **1005**, 083 (2010) [arXiv:1003.1302 [hep-th]].

- [8] E. D'Hoker and P. Kraus, "Magnetic Field Induced Quantum Criticality via new Asymptotically AdS_5 Solutions," *Class. Quant. Grav.* **27**, 215022 (2010) [arXiv:1006.2573 [hep-th]].
- [9] E. D'Hoker and P. Kraus, "Charged Magnetic Brane Correlators and Twisted Virasoro Algebras," *Phys. Rev. D* **84**, 065010 (2011) [arXiv:1105.3998 [hep-th]].
- [10] K. Jensen, A. Karch and E. G. Thompson, "A Holographic Quantum Critical Point at Finite Magnetic Field and Finite Density," arXiv:1002.2447 [hep-th].
- [11] D. Anninos, W. Li, M. Padi, W. Song and A. Strominger, "Warped AdS_3 Black Holes," *JHEP* **0903**, 130 (2009) [arXiv:0807.3040 [hep-th]].
- [12] G. Compere and S. Detournay, "Boundary conditions for spacelike and timelike warped AdS_3 spaces in topologically massive gravity," *JHEP* **0908**, 092 (2009) [arXiv:0906.1243 [hep-th]].
- [13] E. D'Hoker and P. Kraus, "Magnetic Brane Solutions in AdS ," *JHEP* **0910**, 088 (2009) [arXiv:0908.3875 [hep-th]].
- [14] E. D'Hoker and P. Kraus, "Charged Magnetic Brane Solutions in AdS_5 and the fate of the third law of thermodynamics," arXiv:0911.4518 [hep-th].
- [15] L. J. Romans, "The $F(4)$ Gauged Supergravity In Six-dimensions," *Nucl. Phys. B* **269**, 691 (1986).
- [16] R. Gregory, S. L. Parameswaran, G. Tasinato and I. Zavala, "Lifshitz solutions in supergravity and string theory," *JHEP* **1012**, 047 (2010) [arXiv:1009.3445 [hep-th]].
- [17] H. Braviner, R. Gregory and S. F. Ross, "Flows involving Lifshitz solutions," *Class. Quant. Grav.* **28**, 225028 (2011) [arXiv:1108.3067 [hep-th]].
- [18] N. Seiberg, "Five-dimensional SUSY field theories, nontrivial fixed points and string dynamics," *Phys. Lett. B* **388**, 753 (1996) [hep-th/9608111].
- [19] S. Kachru, X. Liu and M. Mulligan, "Gravity Duals of Lifshitz-like Fixed Points," *Phys. Rev. D* **78**, 106005 (2008) [arXiv:0808.1725 [hep-th]].
- [20] S. A. Hartnoll and L. Huijse, "Fractionalization of holographic Fermi surfaces," arXiv:1111.2606 [hep-th].
- [21] E. D'Hoker, P. Kraus and A. Shah, "RG Flow of Magnetic Brane Correlators," *JHEP* **1104**, 039 (2011) [arXiv:1012.5072 [hep-th]].

- [22] A. Almuhairi, “AdS₃ and AdS₂ Magnetic Brane Solutions,” arXiv:1011.1266 [hep-th].
- [23] A. Almuhairi and J. Polchinski, “Magnetic AdS \times R²: Supersymmetry and stability,” arXiv:1108.1213 [hep-th].
- [24] A. Donos, J. P. Gauntlett and C. Pantelidou, “Spatially modulated instabilities of magnetic black branes,” JHEP **1201**, 061 (2012) [arXiv:1109.0471 [hep-th]].
- [25] A. Donos, J. P. Gauntlett and C. Pantelidou, “Magnetic and electric AdS solutions in string- and M-theory,” arXiv:1112.4195 [hep-th].
- [26] A. Almheiri, “Magnetic AdS₂ \times R² at Weak and Strong Coupling,” arXiv:1112.4820 [hep-th].